

A More Ambitious Proton EDM Prototype
Richard Talman
Laboratory for Elementary-Particle Physics
Cornell University

EDM Task Force, Juelich
19 January, 2018

2 Outline

Reduced energy EDM ring on COSY footprint

Spin tunes in superimposed electric and magnetic fields

IRON-FREE stripline magnetic field

Frozen spin operation with weak vertical magnetic field

Proton EDM measurement in ring matched to COSY footprint

Low energy p-helium and p-carbon polarimetry candidates

Electron EDM measurement in ring matched to COSY footprint

3 Field Transformations

The dominant fields in an electric storage ring are radial lab frame electric field $\mathbf{E} = -E\hat{\mathbf{x}}$ and/or vertical lab magnetic field $\mathbf{B} = B\hat{\mathbf{y}}$. Transverse proton rest frame field vectors \mathbf{E}' and \mathbf{B}' , and longitudinal components E'_z and B'_z , are related by

$$\mathbf{E}' = \gamma(\mathbf{E} + \boldsymbol{\beta} \times c\mathbf{B}) = -\gamma(E + \beta cB)\hat{\mathbf{x}} \quad (1)$$

$$\mathbf{B}' = \gamma(\mathbf{B} - \boldsymbol{\beta} \times \mathbf{E}/c) = \gamma(B + \beta E/c)\hat{\mathbf{y}} \quad (2)$$

$$E'_z = E_z, \quad (3)$$

$$B'_z = B_z. \quad (4)$$

Even if lab magnetic field $B = 0$, in the proton rest frame $\mathbf{B}' \neq 0$. Except in the nonrelativistic regime, the magnetic field in the particle rest frame (and hence the induced spin precessions) are comparable in laboratory electric and magnetic fields.

4 All-electric proton frozen spin parameters

$$\begin{aligned}c &= 2.99792458e8 \text{ m/s} \\m_p c^2 &= 0.93827231 \text{ GeV} \\ \gamma_0 &= 1.248107349 \\ \mathcal{E}_0 &= \gamma_0 m_p c^2 = 1.171064565 \text{ GeV} \\ K_0 &= \mathcal{E}_0 - m_p c^2 = 0.232792255 \text{ GeV} \\ p_0 c &= 0.7007405278 \text{ GeV} \\ \beta_0 &= 0.5983790721 \\ G &= 1.7928474\end{aligned}\tag{5}$$

the last of which is the proton anomalous magnetic moment G . For mnemonic purposes it is enough to remember $\beta_0 \approx 0.6$, $p_0 c \approx 0.7 \text{ GeV}$ and $\gamma_0 \approx 1.25$.

5 Reduced energy EDM ring on COSY footprint

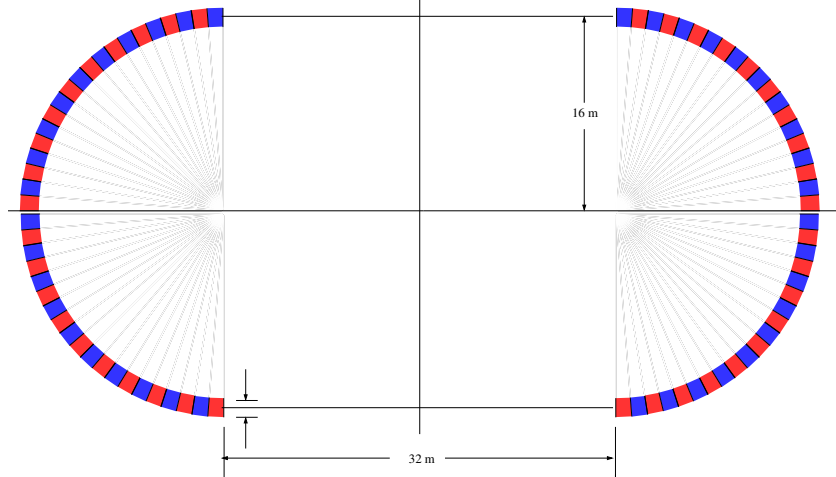


Figure 1: (Reduced energy) proton EDM ring more or less matched to the COSY footprint. Superimposed magnetic field (0.02171 T) is required because the proton 84 MeV energy is less than the 233 MeV magic energy required to freeze the spins in an all-electric ring.

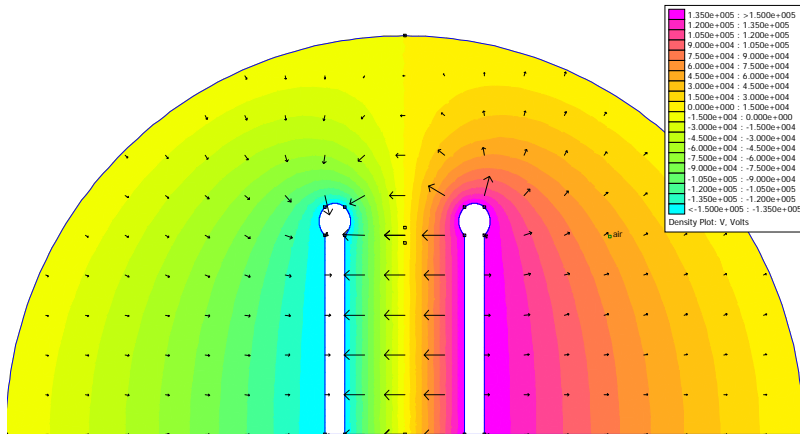


Figure 2: The top 5 cm of cylindrical electrodes is shown. The electrode height can be increased without altering the electric field. A tentative electrode height is $H_{\text{electrode}} = 0.19$ m. Bulb-shaped edges maximize the good field volume. Less obvious pole shaping will also be present to produce deviation from purely cylindrical electric field.

7 Proton parameter table

Table 1: Parameters for maximum bend radius prototype on COSY footprint. The values in this, and subsequent tables are only crude, because the short drift lengths are being neglected. Since transverse dynamics is purely geometrical, kinematic quantities such as speed and energy, and even particle type, do not enter,

parameter	symbol	unit	value
arcs			2
cells/arc	N_{cell}		20
bend radius	r_0	m	16
short drift length	L_D	m	1.2
accumulated drift length		m	83.2
circumference	\mathcal{C}	m	184
field index	m		± 0.2
horizontal beta (max)	β_x	m	57
vertical beta	β_y	m	1050
(outside) dispersion	D_x^O	m	9.7
horizontal tune	Q_x		1.81
vertical tune	Q_y		0.028
protons per bunch	N_p		1.0×10^8
horz. emittance	ϵ_x	μm	?
vert. emittance	ϵ_y	μm	?
(outside) mom. spread	$\Delta p^O/p_0$		$\pm 2 \times 10^{-4}$
(inside) mom. spread	$\Delta p^I/p_0$		$\pm 2 \times 10^{-5}$

8 Tune Advances

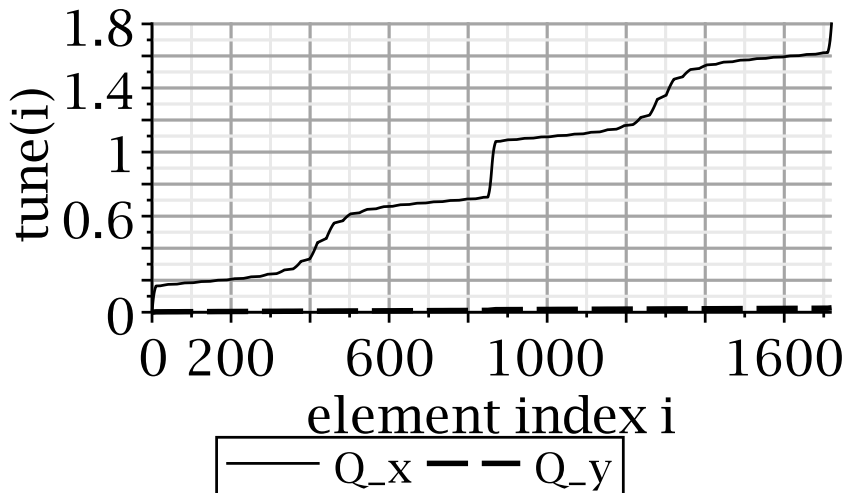


Figure 3: $Q_x = 1.81$, $Q_y = 0.002$

9 Horizontal beta function β_x

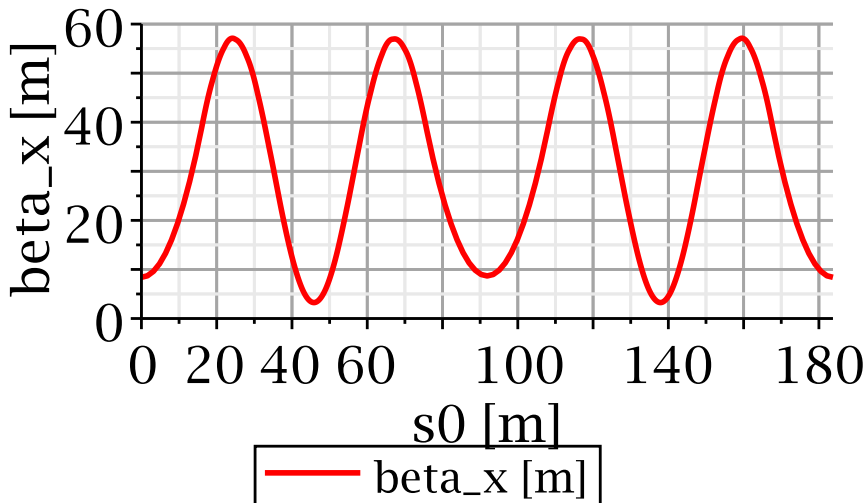


Figure 4: $\beta_x^{\max} = 57$ m.

10 Vertical beta function β_y

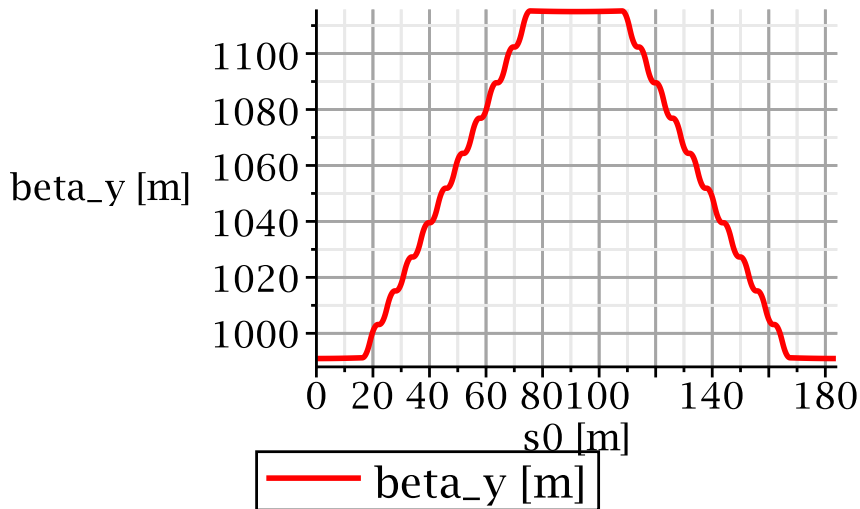


Figure 5: $\beta_y \approx 1050$ m.

11 Dispersion function

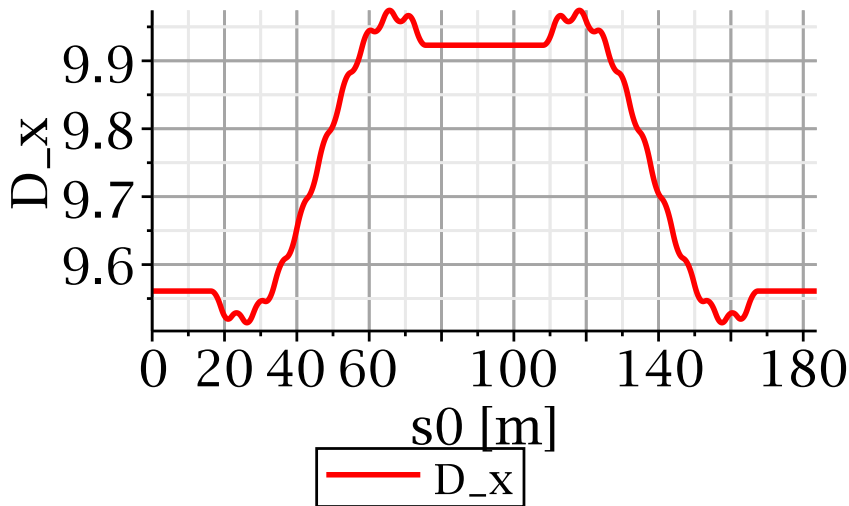


Figure 6: $D \approx 9.7$ m.

12 Spin tunes in electric and magnetic fields

The “spin tune” Q_E in an electric field is given by

$$Q_E = G\beta^2\gamma - \frac{1}{\gamma} = G\gamma - \frac{G+1}{\gamma}. \quad (6)$$

The “spin tune” Q_M in an magnetic field is given by

$$Q_M = G\gamma. \quad (7)$$

For the proton, $G = 1.792847356$. Notice that

$$Q_E = Q_M - \frac{G+1}{\gamma}. \quad (8)$$

For the electron, $|G| \approx 0.001$ and $Q_E \approx Q_M = G\gamma$ for any realistically high energy electron storage ring.

13 Superimposed electric and magnetic fields

For circular motion at radius r_0 in superimposed electric and magnetic field the centripetal force is $eE + e\beta cB$. By Newton's law

$$\frac{(pc/e)\beta}{r_0} = E + \beta cB. \quad (9)$$

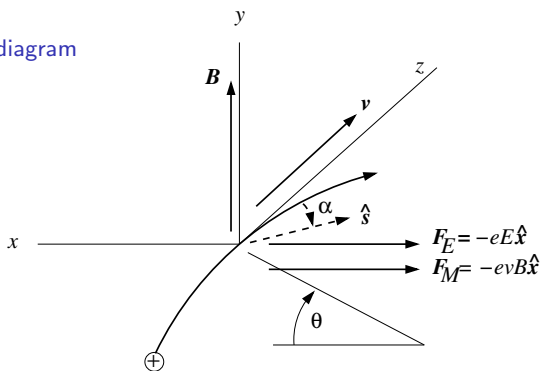
Dividing out a common factor, the centripetal force can be expressed as electric and magnetic bending fractions η_E and η_M ;

$$\eta_E = \frac{r_0}{pc/e} \frac{E}{\beta}, \quad \eta_M = \frac{r_0}{pc/e} cB, \quad \text{where } \eta_E + \eta_M = 1. \quad (10)$$

- ▶ We assume $E > 0$ and $\eta_E > 0$, but without necessarily requiring η_M to also be positive. We also assume $G > 0$ (which includes electron and proton, but not deuteron and helion.)
- ▶ But, together, the η 's must sum to 1; i.e. B can be negative, providing centrifugal rather than centripetal force.
- ▶ Expressed in terms of the eta's, the fields are given by

$$E = \frac{pc/e}{r_0} \beta \eta_E, \quad cB = \frac{pc/e}{r_0} \eta_M. \quad (11)$$

14 Vector force diagram



- ▶ For a positive particle moving away, along the positive-z axis, with increasing global angle θ , for electric field $\mathbf{E} = -E\hat{x}$ and magnetic field $\mathbf{B} = B\hat{y}$ to sum constructively, causing the particle to veer to the right (in the negative-x direction), requires both E and B to be positive.
- ▶ For positive spin tune Q_s the spin precession angle α increases with increasing θ ; i.e.

$$\frac{d\alpha}{d\theta} = Q_s. \quad (12)$$

15 Superimposed electric and magnetic bending—protons

We require the resulting spin tune Q_{EM} to vanish;

$$Q_{EM} = \eta_E Q_E + (1 - \eta_E) Q_M = 0. \quad (13)$$

Solving for η_E ,

$$\eta_E = \frac{G}{G+1} \gamma^2. \quad (14)$$

For example, try $\gamma = 1.25$;

$$\eta_E = \frac{1.7926}{2.7926} \times 1.25^2 = 1.000, \quad (15)$$

which agrees with the “magic” proton value, for which no magnetic bending is required.

In the non-relativistic limit $\gamma = 1$ and

$$\eta_E^{\text{NR}} = \frac{1.7926}{2.7926} = 0.6419 \approx \frac{2}{3}. \quad (16)$$

16 Magnetic field in current-carrying stripline

A (fairly weak) uniform magnetic field B can be produced by current I_B flowing in a stripline of width w . To produce magnetic bending fraction η_M (using Ampère's law) the current is

$$I_B = \frac{B}{\mu_0} w = \frac{\rho c/e}{r_0} \frac{w}{\mu_0 c} \eta_M, \quad (17)$$

where $\mu_0 c = Z_0 = 377 \Omega$ is the free space impedance. The I_B/E ratio then, for example with 1/3 of the bending being magnetic, for $K = 82$ MeV protons, is

$$\frac{I_B}{E} = \frac{w}{377 \Omega} \frac{1}{\beta} \frac{\eta_M}{\eta_E} \stackrel{\text{e.g.}}{=} \frac{0.19}{377} \frac{1}{0.39} \frac{1}{2} = 0.65 \times 10^{-3}. \quad (18)$$

- ▶ To turn 82 MeV protons on a 20 m radius requires electric field $E = 8 \times 10^6$ V/m.
- ▶ Produced by current $(0.65 \times 10^{-3}) \times (8 \times 10^6) = 5200$ A, the magnetic bending would be roughly half as great as this electric bending, and the ring radius could therefore be about 14 m.
- ▶ and the proton spins would be approximately frozen.
- ▶ See Figure.

17 Q_E and Q_M spin tune plots

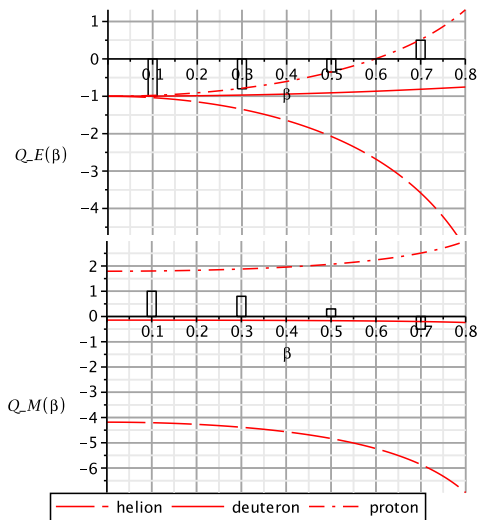


Figure 7: The bar heights roughly indicate, depending on β , how much magnetic bending, relative to electric bending, is needed to “freeze” proton spins.

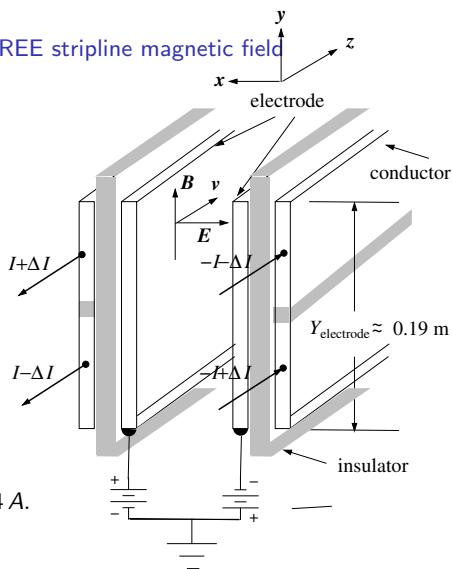
18 Reduced energy proton EDM with IRON-FREE stripline magnetic field

At least in principle, the required magnetic field can be produced by stripline currents shown in the figure. For not very relativistic protons the magnetic force needs to be approximately half the electric force. For example, for $\beta_p = 0.126$

$$B = \frac{E/c}{2\beta_p} = \frac{5 \times 10^6 / 3 \times 10^8}{2 \times 0.126} = 0.0661 \text{ T} \quad (19)$$

The stripline current producing this magnetic field is

$$I = \frac{B}{\mu_0} Y_{\text{electrode}} = \frac{0.0661}{4\pi \times 10^{-7}} 0.19 = 9994 \text{ A}. \quad (20)$$



Superimposed electric and magnetic fields.

Weakest-possible vertical focusing can be provided by ΔI current imbalance (as shown). Up/down current (milliamp scale) imbalance can provide radial magnetic field compensation.

19 Frozen spin 233 MeV proton operation with weak magnetic field

- ▶ 233 MeV ($\beta = 0.6$) proton spins are frozen in an electrostatic storage ring. But a purely electrostatic storage ring may be subject to regenerative vacuum degradation causing the beam lifetime to be too short for sensitive EDM measurement.
- ▶ Steering ions in a direction perpendicular to the electric field by superimposing a weak vertical magnetic field ΔB might help to suppress this loss mechanism.
- ▶ By Eq. (14), a change $\Delta\gamma$ in beam energy associated with a non-vanishing magnetic fraction $\Delta\eta_M$ needs to be compensated by a change $\Delta\eta_E = -\eta_M$, such that

$$-\eta_M = \frac{G}{G+1} (\gamma_0 + \Delta\gamma)^2 - \frac{G}{G+1} \gamma_0^2 \approx \frac{2G\gamma_0^2}{G+1} \frac{\Delta\gamma}{\gamma_0} = \frac{2\Delta\gamma}{\gamma_0}. \quad (21)$$

20 Frozen spin 233 MeV proton operation with weak magnetic field (continued)

For example, with magic beta value at its nominal (full energy) value of $\beta_0 = 0.6$, suppose the electric field is increased from 5×10^6 to 6×10^6 V/m. This is a twenty percent change that would increase the magic gamma value by ten percent. Re-arranging Eq. (19), the magnetic field required to cancel the steering change is

$$B = -\frac{\Delta E/c}{\beta_p} = -\frac{10^6}{0.6 \times 3 \times 10^8} = -0.0055 \text{ T.} \quad (22)$$

The required longitudinal current would then be given by Eq. (20);

$$I = \frac{B}{\mu_0} Y_{\text{electrode}} = \frac{0.0055}{4\pi \times 10^{-7}} 0.19 = 851 \text{ A.} \quad (23)$$

- ▶ This current is as small as it is both because of the nearness to the all-electric magic parameter value.
- ▶ However, the given magnetic field might not be strong enough to influence beam dynamics significantly.

21 Proton EDM measurement in ring matched to COSY footprint

REDUCED ENERGY PROTON EDM RING ON COSY FOOTPRINT

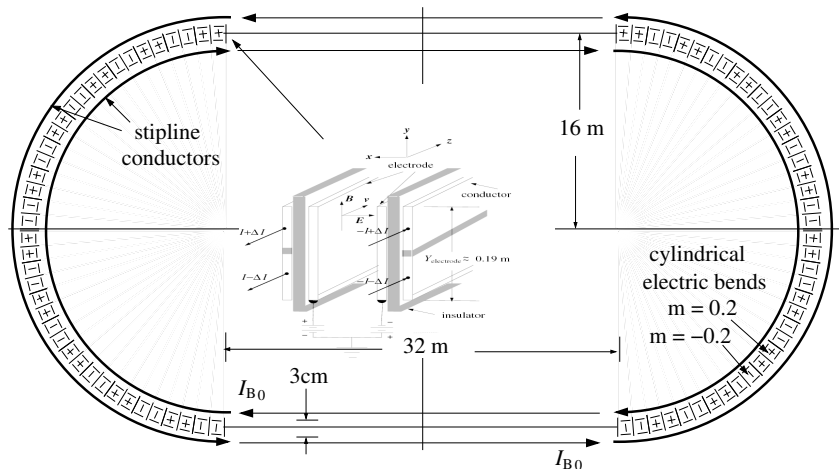


Figure 8: (Reduced energy) proton EDM ring more or less matched to the COSY footprint. Superimposed magnetic field (0.02171 T) is required because the proton 84 MeV energy is less than the 233 MeV magic energy required to freeze the spins in an all-electric ring.

22 Proton EDM prototype options parameter table

The table below gives parameters for possible proton EDM prototype rings described in these lectures. The final column gives parameters for the 2011 Brookhaven proton EDM proposal[7].

Table 2: Some values are only crude because the short drift lengths are being neglected. Also the electrode height $w = 0.19$ m has not been matched to the gap width in the large bore case.

parameter	symbol	unit	COSY footprint		pEDM -PROTO	pEDM-BNL
			max. energy	large bore		
circumference	C	m	183		40	500
bend radius	r_p	m	16		3	40
momentum $\times c$	$p_0 c$	GeV	0.4007	0.2804		0.70074
kinetic energy	K	MeV	82	41	7.5	233
proton beta	β_0		0.39279	0.28632		0.6
proton velocity	v_p	m/s	1.177547e8	0.85838e8	3.77e7	1.8e8
proton gamma	γ_0		1.248107	1.04369		1.25
revolution period	T_1	μs	1.56257	2.1436		2.78
elec. bend frac.	η_E		0.75905	0.6993	1.0	1.0
electric field	E	MV/m	7.4676	3.5087	5	10
electrode gap	gap	cm	3	10	3	3
electrode voltage	V_0	KV	± 112	± 176		± 157
magn. bend frac.	η_M		0.24094	0.3007	0.0	0.0
"magic" magn. field	B_0	T	0.020130	0.01758		
"magic" current	I_{B0}	A	3044	2658		

23 Low energy p-helium and p-carbon polarimetry candidates

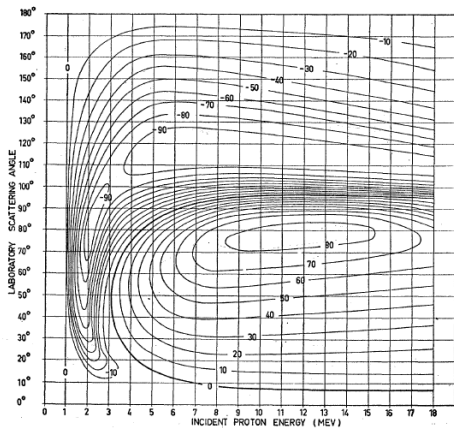


FIG. 2. Contour plot of percent polarization in proton-helium scattering as a function of incident proton energy and laboratory scattering angle.

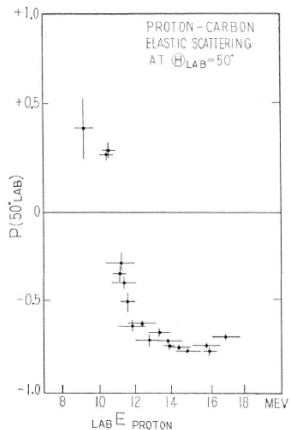


Figure 3
The energy dependence of $P(50^\circ_{LAB})$.

24 Electron EDM measurement in ring matched to COSY footprint

- ▶ (As Bill Morse first emphasized) superimposed magnetic bending permits the electron spins to be frozen over a large parameter range, permitting controlled investigation of systematic errors.
- ▶ Above $\gamma_e = 30$ one can increase the electric field more or less arbitrarily and cancel most of the bending magnetically to preserve frozen spins. In effect the magnetic contribution to the spin tune is then negative.

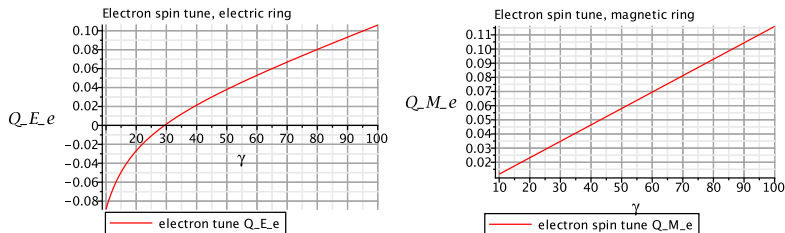


Figure 9: The “magic” value is $\gamma_e \approx 30$, but this can be changed by a large factor by superimposing magnetic field on the electric bending field.

25 Superimposed electric and magnetic bending—electrons

- ▶ Spin tunes in electric and magnetic fields are related by

$$Q_E = Q_M - \frac{G + 1}{\gamma}. \quad (24)$$

- ▶ For the electron, $|G| \approx 0.001$ and $Q_E \approx Q_M = G\gamma$ for any realistically high energy electron storage ring.
- ▶ With η_E the electric bending fraction, and η_M the magnetic bending fraction, we require the resulting spin tune Q_{EM} to vanish;

$$Q_{EM} = \eta_E Q_E + (1 - \eta_E) Q_M = 0. \quad (25)$$

- ▶ For electrons $G = 0.001159652$. Solving for η_E ,

$$\eta_E = \frac{G}{G + 1} \gamma^2 \approx 0.001159 \gamma^2; \quad \eta_M = 1 - G\gamma^2 / (G + 1) \approx 1 - 0.001159 \gamma^2. \quad (26)$$

- ▶ For purely electric bending $\eta_M = 0$ and

$$\gamma_{\text{magic}} = \sqrt{\frac{G + 1}{G}} = \sqrt{\frac{1.001159652}{0.001159652}} = 29.382. \quad (27)$$

26 Electron spin tunes in electric and magnetic rings

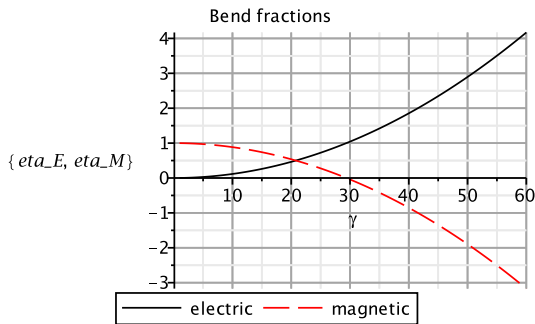


Figure 10: Electron spin tunes in electric and magnetic rings. By superimposing electric and magnetic bending fields the frozen spin condition can be satisfied for arbitrary electron energy.







- ▶ For $\gamma < 30$ both η_E and η_M are positive, meaning that both electric and magnetic forces are centripetal.
- ▶ But for $\gamma > 30$ both η_M and B are negative, as is required for the spins to remain frozen.
- ▶ Note, though, that the electric field in the electron rest frame continues to increase with increasing γ , as required to provide the increased bending force to keep the particle on a 16 m radius circle.









27 Parameters for frozen spin electron EDM scan

Table 3: Some values are only crude because the short drift lengths are being neglected.

parameter	symbol	unit	COSY footprint				
circumference	C	m	183				
bend radius	r_p	m	16				
short drift length	L_D	m	1.2				
accum. drift length		m	83.2				
momentum $\times c$	$p_0 c$	GeV	0.00749	0.0106	0.0150	0.0212	0.0300
kinetic energy	K	MeV	6.70	10.10	14.50	20.72	29.5
electron beta	β_e		0.9977	0.9988	0.9994	0.9997	0.9998
electron gamma	γ_e		14.69	20.77	29.38	41.55	58.76
elec. bend frac.	η_E		0.25	0.5	1.0	2.0	4.0
electric field	E	MV/m	0.1173	0.3317	0.937	2.65	7.507
electrode gap	gap	cm	3	3	3	3	3
gap voltage	V_0	KV	3.52	9.95	28.1	79.62	225
magn. bend frac.	η_M		0.75	0.5	0.0	-1.0	-3.0
"magic" magn. field	B_0	T	0.00117	0.00110	0.0	-0.00442	-0.0188
"magic" current	I_{B0}	A	177.06	167.13	0.0	-669.1	-2839

- ▶ For electron EDM measurement, with magic energy 14.5 MeV, bend radius $r_0 = 16$ m may seem unnecessarily large.
- ▶ Note, though, that the electric field can be increased (to its maximum possible value) and the magnetic field increased correspondingly—the required currents I_B do not seem excessive.
- ▶ This nearly doubles the (already large) EDM precession induced by the electric field.

-  R. Talman, *The Electric Dipole Moment Challenge*, IOP Publishing, 2017
-  D. Eversmann et al., *New method for a continuous determination of the spin tune in storage rings and implications for precision experiments*, Phys. Rev. Lett. **115** 094801, 2015
-  N. Hempelmann et al., *Phase-locking the spin precession in a storage ring*, P.R.L. **119**, 119401, 2017
-  R. Talman, J. Grames, R. Kazimi, M. Poelker, R. Suleiman, and B. Roberts, *The CEBAF Injection Line as Stern-Gerlach Polarimeter*, Spin-2016 Conference Proceedings, 2016
-  R. Talman, LEPP, Cornell University; B. Roberts, University of New Mexico; J. Grames, A. Hofler, R. Kazimi, M. Poelker, R. Suleiman; Thomas Jefferson National Laboratory; *Resonant (Longitudinal and Transverse) Electron Polarimetry*, 2017 International Workshop on Polarized Sources, Targets and Polarimetry, KAIST, Republic of Korea, 2017
-  R. Li and P. Musumeci, *Single-Shot MeV Transmission Electron Microscopy with Picosecond Temporal Resolution*, Physical Review Applied 2, 024003, 2014

-  Storage Ring EDM Collaboration, *A Proposal to Measure the Proton Electric Dipole Moment with 10^{-29} e-cm Sensitivity*, October, 2011
-  V. Anastassopoulos, et al. *Search for a permanent electric dipole moment of the deuteron*, AGS proposal, 2008
-  G. Guidoboni et al., *How to reach a thousand second in-planepolarization lifetime with 0.97 GeV/c deuterons in a storage ring*, P.R.L. **117**, 054801, 2016
-  M. Plotkin, *The Brookhaven Electron Analogue, 1953-1957*, BNL-45058, December, 1991
-  S.P. Møller, *ELISA—An Electrostatic Storage Ring for Atomic Physics*, Nuclear Instruments and Methods in Physics Research A 394, p281-286, 1997
-  S. Møller and U. Pedersen, *Operational experience with the electrostatic ring, ELISA*, PAC, New York, 1999
-  S. Møller et al., *Intensity limitations of the electrostatic storage ring, ELISA*, EPAC, Vienna, Austria, 2000
-  Y. Senichev and S. Møller, *Beam Dynamics in electrostatic rings*, EPAC, Vienna, Austria, 2000



A. Papash et al., *Long term beam dynamics in Ultra-low energy storage rings*, LEAP, Vancouver, Canada, 2011



R. von Hahn, et al. *The Cryogenic Storage Ring*, arXiv:1606.01525v1 [physics.atom-ph], 2016



j. Ullrich, et al., *Next Generation Low-Energy Storage Rings, for Antiprotons, Molecules, and Atomic Ions in Extreme Charge States*,



Loss of protons by single scattering from residual gas is discussed in detail in a paper Frank Rathmann drew to my attention: C. Weidemann et al., *Toward polarized anti-protons: Machine development for spin-filtering experiments*, PRST-AB **18**, 0201, 2015